Proceedings of the Twentieth (2010) International Offshore and Polar Engineering Conference
Beijing, China, June 20–25, 2010

ISBN 978-1-880653-77-7 (Set); ISSN 1098-6189 (Set); www.isope.org

On the Capacity and Deformation of Bucket Foundation under Dynamic Loadings

Chi Li
Inner Mongolia University of Technology
Huhhot, P. R. China

Xiaobing Lu & *Shuyun Wang*
Institute of mechanics, Chinese Academy of Science
Beijing, P. R. China

ABSTRACT

Simplified numerical model is built according to centrifugal experimental results. The liquefaction degree and deformation of sand sediment around bucket foundation are simulated. Effects of main factors are investigated. A spring model for modeling the capacity degradation of bucket foundation is presented in which sand resistance is modeled by uncoupled, non-linear sand springs. When the liquefaction degree is 0.9 near the surface and is only 0.06 at the bottom of sand sediment, the capacity degradation of bucket is 12%, whereas it is 17% in centrifugal experiments. Deformation of sand sediment increases with the increase of loading amplitude and skeleton's elastic modulus and the decrease of frequent. The maximum vertical deformation on the surface of sediment is 0.25 times of bucket depth away from loading side. The maximum horizontal deformation is on the loading side.

KEY WORDS: Bucket foundation; dynamic loading; liquefaction degree; capacity degradation.

INTRODUCTION

As a new type and removable offshore structure, bucket foundation is extensively used in ocean engineering because of their simplicity, reliability and economical. Despite some studies on the static capacity of bucket foundation have been done (Aas and Andersen, 1992; Sherif, 1999; Tjelta et al., 1990; Randolph and House, 2002), long-term bearing capacity of bucket foundation have not clarified, e.g. the capacity degradation under dynamic loading. Some methods for the evaluation of long-term bearing capacity under cyclic loads have been presented which can serve as good references for us (Prevost, 1981; Marr, 1981; Andersen, 1988; Andersen, 1993; David, 1982).

Experimental study is crucial for deep understanding of the bearing capacity of bucket foundation. Cyclic triaxial experiments and large-scale model experiments were carried out to study saturated soft clay's cyclic strength and bearing capacity of bucket foundations in it, based on which a method for estimating the bearing capacity is presented (Wang and Liu, 1998; Li and Wang, 2005). Centrifuge experiments were carried to study the responses (softening, liquefaction) of sand sediment and bucket foundations dynamic loadings (Lu et al., 2003; Wang et al., 2006). The above studies showed that liquefaction or softening of sand sediment occurring under dynamic loadings.
In this paper, numerical simulations are carried out based on the centrifuge results in the literatures of Lu et al. (2007) and Zhang et al. (2007) and Wang et al. (2006). The relationship between liquefaction degree and degradation of bucket foundation's bearing capacity, and the deformation of sediment around the bucket foundation are analyzed.

INTRODUCTION OF CENTRIFUGAL EXPERIMENTAL RESULTS

Layout of Experiment

Centrifugal experiments have been carried out in the 50*g-t* geotechnical centrifuge in Tsinghua University before, the maximum centrifugal acceleration is 250*g* (Zhang et al., 2007; Wang et al., 2006, Lu et al., 2007). The inner size of the model box is 600*mm*×350*mm*×350*mm*. Fine sand is adopted in experiments whose specific gravity is 2.69, the average diameter is 0.14*mm*, and the permeability coefficient is 5×10^{-3}*mm*/*s*.

The inner and outer diameters of the bucket are 60*mm* and 62*mm*, respectively. The net depth of the bucket is 70*mm*, 72*mm*, and 48*mm*, the thickness of the cap is 2*mm*. Two LVDTs were placed on the top of bucket to measure the horizontal and vertical displacements respectively, two LVDTs were placed on the surface of sediment to measure the settlement. Ten PDCR81 type PPTs were placed in two types shown in Fig 1.

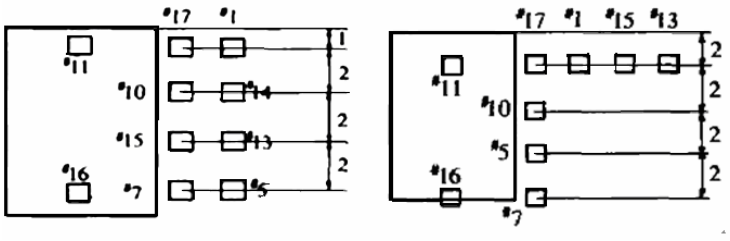

(a) (b)
Fig.1 Two arrangement forms of PPT

The loading frequency used in centrifuge experiments was 1.0*Hz*. Fig.2 shows the force applied on the bucket foundation in the beginning stage and the later stage. It can be seen that the bearing capacity of bucket decreases about 17% after the top sand liquefied.

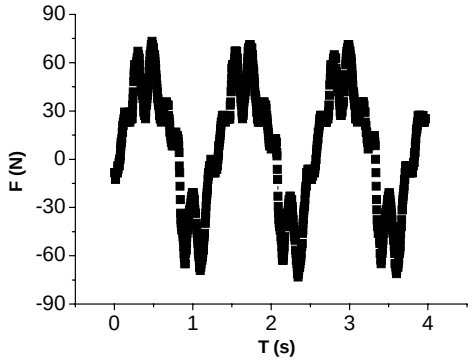

(a) beginning stage

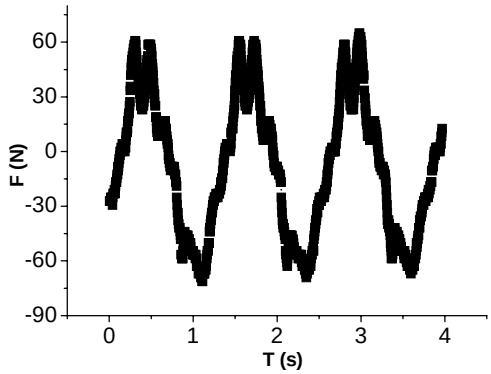

(b) last stage

Fig.2 Dynamic load applied on the bucket

Centrifugal Experimental Results

Experimental results show that the excess pore pressure increases quickly in the beginning, and then decreases gradually. The liquefaction degree *FL* (the ratio of excess pore water pressure (*u*) to initial vertical effective stress (*σ'*), e.g. *FL =u/σ'*.) varies with loading amplitude (Fig.3). Figs.4 (a) (b) shows the distribution of liquefaction degree in vertical and horizontal directions respectively. It is shown that the development of pore pressure is faster at the upper part. The upper part has liquefied (liquefaction degree approach 1.0), while it is only 0.08 at the bottom. In horizontal direction, when loading amplitude is 60N, the sediment liquefies at the position 0.2m away from the side wall of bucket, while the liquefaction degree is only 0.4 at the position 1.4m away from the side wall of bucket. This is why the bucket foundation still has large bearing capacity under long-term dynamic loadings.

NUMERICAL SIMULATION

Numerical Model

Coulomb friction cell were often used to model the interaction between the bucket and the sand are simulated (Wang et al., 2005; Li et al., 2005; Li et al., 2006). Although it is effective in static conditions, the coulomb friction cell is not able to model dynamical responses since the direction of dynamic loadings is to and fro (Fast Lagrangian Analysis of Continua, 2005). According to the centrifugal experimental results, the bucket and the sand inside the bucket may be thought as a rigid body compared with the sand sediment around it.

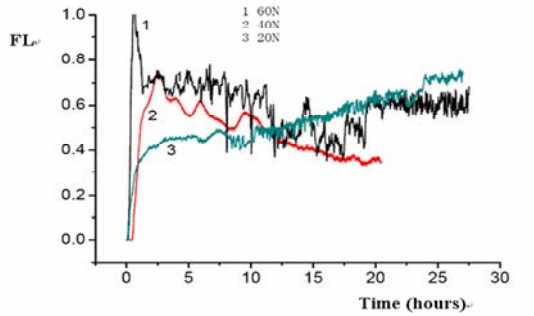

Fig.3 Liquefaction degree vs. loading amplitude (NO.10 PPT)

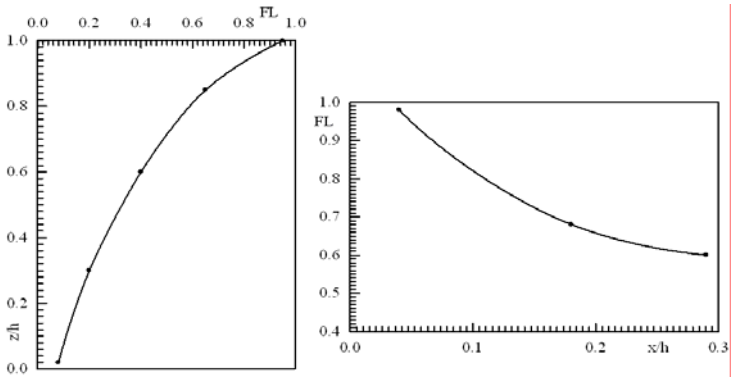

(a) in depth direction (b) in horizontal direction

Fig.4 Experimental results of liquefaction degree distribution

The software FLAC3D is used in this section for numerical simulation. The numerical model can be described as follows: The sand sediment on the right of bucket wall is assumed to be finite in depth but semi-infinite in horizontal direction. It is assumed as a plane strain problem in x-z plane, the simplified numerical network is shown in Fig.5 (a).

The boundary effects in dynamic numerical simulation are important, because they can lead to the reflection of wave. To avoid this, absorbing boundaries on the right side of sediment are used in this paper. The top of sediment is free and the bottom is impermeable and vertically fixed.

The calculation procedures are as follows: firstly, the initial earth stress is balanced gradually by confining stress state. Secondly, quite condition is adopted at the right side, at the bottom it is still fixed. Dynamic loadings are applied on the left side of sediment. Dynamic load is a sine function of displacement applied on the left side of sediment. The red line shown in Fig.5 (b) denotes the loading series on the surface of sediment, the maximum amplitude is 16*cm* on the surface; while the green line denotes that in the middle and the amplitude is 10*cm;* the amplitude is zero at the bottom. The load frequency is 1.0*Hz*.

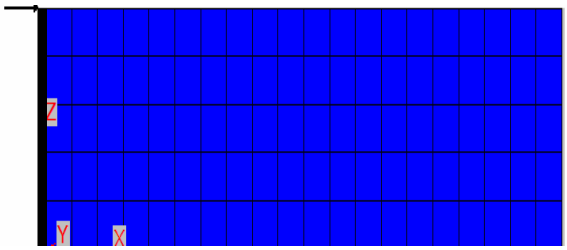

(a) Plane-strain model

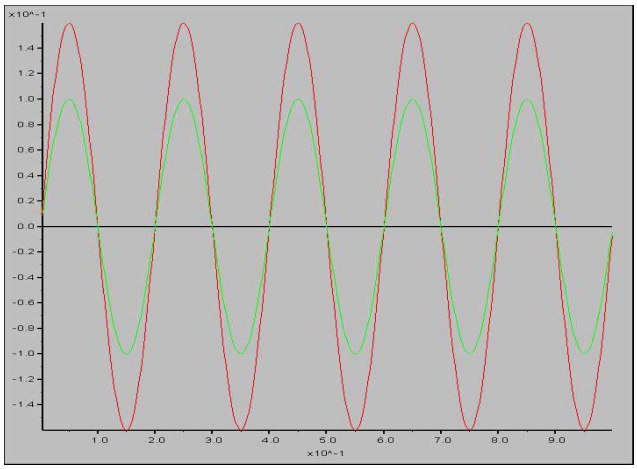

(b) Equivalent dynamic load series (load frequency is 1.0*Hz*)

Fig.5 Simplified Numerical model

Parameters Used in Numerical Simulation

The saturated sand is taken as two-phase media: sand skeleton and pore water. During the calculation for initial earth stress, the Mohr-Coulomb model is adopted, and the pore water is assumed isotropy elastic. According to the results of cyclic triaxial experiments, the elastic modulus of sand sediment is $4.0\times10^7 pa$, the Poisson's ratio is 0.35, the internal friction angle is 36.5°, the density is $1600 kg/m^3$ and the relative density is 0.54 (Lu et al, 2007). The initial water-head is zero at the surface of sediment. It is impermeable at the bottom. The increase of pore poressure is assumed to satisfy the Finn model (Eqs.(1-3)) (Martin et al., 1975). The Biot's coefficient is 1.0, permeability coefficient is$1.0\times10^{-6} m/s$, the bulk modulus of pore water is $2.0\times10^9 pa$ and initial porosity ratio is 0.40.

According to the Finn model, the strain increment is calculated by Byrne equation shown in Eq.(1)~Eq.(3).

$$\frac{\triangle\varepsilon_{vd}}{\gamma} = c_1 \exp\left(-c_2\left(\frac{\varepsilon_{vd}}{\gamma}\right)\right) \tag{1}$$

$$c_1 = 7600\times\left(Dr\right)^{-2.5} \tag{2}$$

$$c_2 = \frac{0.4}{c_1} \tag{3}$$

in which $\triangle\varepsilon_{vd}$ —plastic volume strain increment, γ —the maximum cyclic shear strain, c_1, c_2 —constants, D_r —relative density of sand

Comparison of Numerical and Experimental Results

To compare the numerical results with experimental results, the load conditions and initial boundary condition are adopted according to the centrifuge experiments (loading amplitude is 60*N*, frequency is 1.0*Hz*). The comparison of liquefaction degree is shown in Table 1 and Table 2. It is shown that the numerical results are close with centrifuge experimental results. The simplified numerical model is reliable.

Table1 Comparison of liquefaction degree in vertical direction

z/h	*FL =u/σ'*	
	centrifuge experiment results	numerical results
0.80	0.95	0.90
0.58	0.24	0.29
0.42	0.10	0.18
0.31	0.08	0.12

Table2 Comparison of liquefaction degree in horizontal direction

x/h	*FL =u/σ'*	
	centrifuge experiment results	numerical results
0.04	1.00	0.90
0.20	0.68	0.56
0.29	0.60	0.55

where: *h* is the height of bucket foundation; *u* is the maximum excess pore pressure; *σ'* is the initial vertical effective stress.

Expansion of Liquefaction Zone

Expansion of liquefied zone and development of liquefaction degree is computed in this section. The development of liquefaction degree along depth and in horizontal direction is shown in Fig.6. It can be seen that the liquefaction degree decreases gradually from the top to the bottom of sediment. The maximum liquefaction degree is 0.9 at the surface of sediment (x=0, z=h), and it is only 0.06 at the bottom (x=0, z=0.2h). In the zone of $0.6h\le z\le h$, liquefaction degree changes obviously. From Fig.6 (b) we can see that the liquefaction degree decreases gradually in horizontal direction from the load side. The liquefaction degree decreases rapidly in the zone x>0.85h. For example, the liquefaction degree is only 0.01 when x=h, while after x>3.0h, it is nearly zero. Therefore, the effected zone in saturated sediment around bucket foundation is in the range of $0\le x\le 0.85h$, $0.6h\le z\le h$ under the adopted loading here.

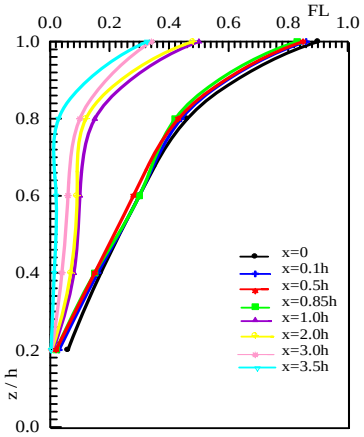

(a)

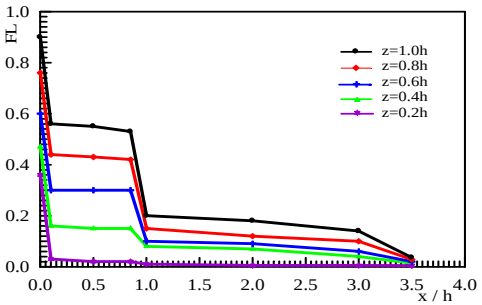

(b)

Fig.6 Numerical results of liquefaction zone expansion

Effects of Factors on Liquefaction Degree

Fig.7 (a) shows the distribution of liquefaction degree along depth at the load side under different dynamic frequencies when the maximum amplitude is 16*cm*. It is shown that when the load frequency is less than 1.0*Hz*, the excess pore pressure accumulates obviously in the whole depth with the increase of frequency. However, when the frequency is more than 1.0*Hz* (show as the dashed line in Fig.7), the accumulation of excess pore pressure only appears near the top surface, while the liquefaction degree at the bottom is very small. Fig 7(b) is the distribution of liquefaction degree along depth under different load amplitudes when the load frequency is 1.0*Hz*. It can be seen that liquefaction degree is large in the zone of $0.6h \le z \le h$. Fig.7 (c) shows the effects of skeleton's elastic modulus. It can be seen that the excess pore pressure increases fast with the decrease of elastic modulus, which causes the fast decrease of the skeleton's strength. For an example, when the elastic modulus decreases from 5×10^8 P*a* to 5×10^7 P*a*, the liquefaction degree on the surface increases rapidly from 0.6 to 0.9.

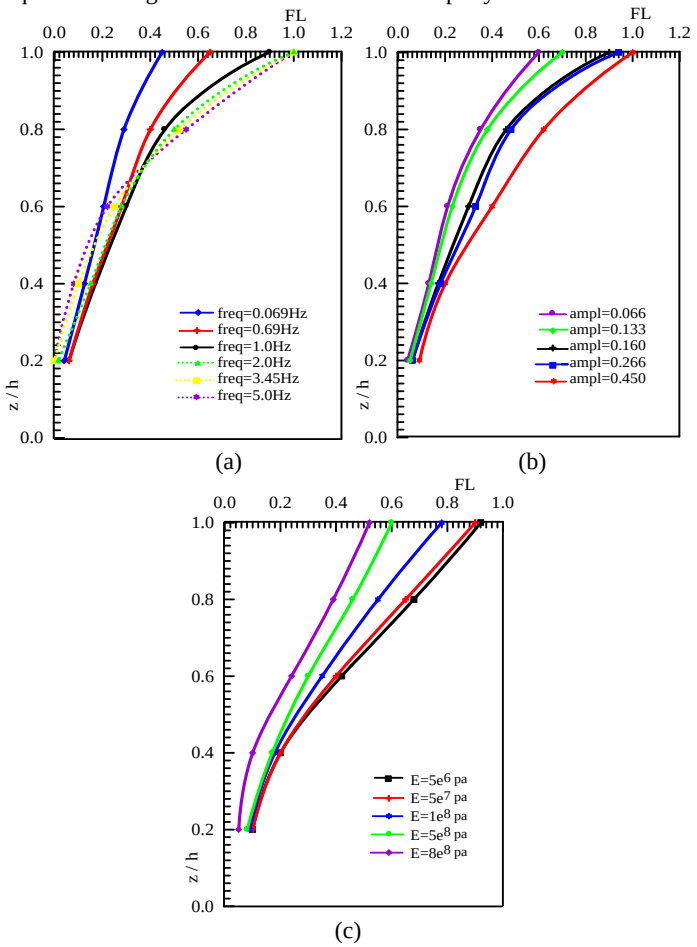

Fig.7 Effects of factors on the distribution of liquefaction degree

Vertical Displacement of Sediment

The vertical displacements (*Sz*) at the surface of sediment ($z=1.0h$) and the lower part ($z=0.2h$) are shown in Fig.8 when the dynamic loading lasts for 1*h*、3*h*、5.5*h*、10*h* and 15*h* respectively. From Fig.8 (a) we can see that the maximum vertical displacement located at 0.25*h*~0.5*h* away from the load side. The vertical displacement decreases gradually in the distance of 0.5*h*~1.0*h*. In the zone $x>h$, the vertical displacements keep as a constant. The vertical displacements in horizontal direction form a "pan-like" zone in the zone $x<h$ which becomes more and more evident. From Fig.8 (b) we can see that the vertical displacements at the lower part is evident in the zone $x<h$. The "pan-like" zone forms an inverted triangle. The maximum value is located at $x=0.25$.

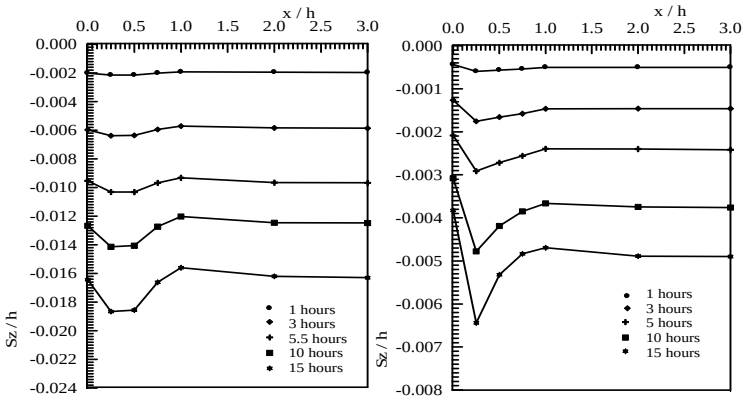

Fig. 8 Distribution of vertical displacement at different time

Horizontal Displacement of Sediment

The horizontal displacement (*Sx*) of the sand sediment reduces gradually in horizon direction. In the zone $x \ge 2h$, the horizontal displacement is so small that it can be neglected. The maximum horizontal displacement is on the left side ($x=0$). Fig.9 (a) shows the displacements at x=0 when the dynamic loadings lasts for 1*h*、3*h*、5*h*、10*h* and 15*h*. Fig.9 (b) shows the horizontal displacements at $x=2.0h$. It can be seen that the horizontal displacement decreases gradually along depth, the maximum is on the top and the minimum is on the bottom.

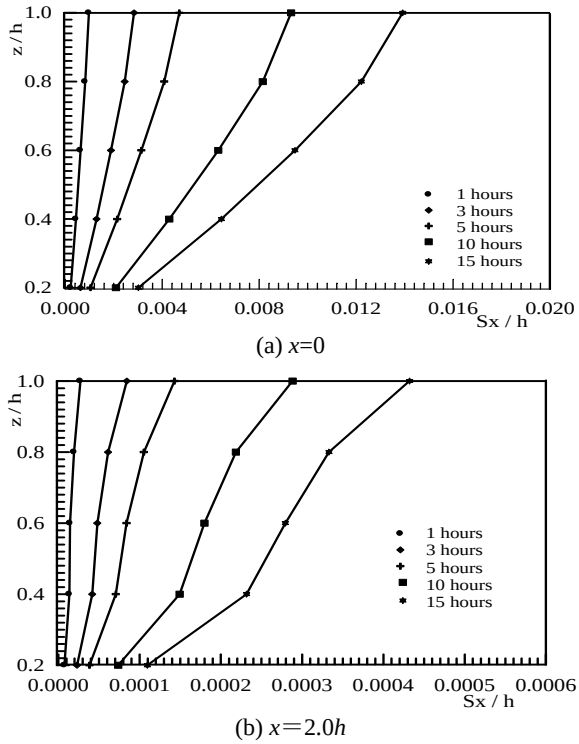

Fig. 9 Distribution of horizontal displacement at different time

Relationship between Displacement and Vibration Time

Fig.10 (a) shows the connections between the maximum vertical displacement at the top or bottom of sediment and the vibration time at x=0.25*h*. It can be seen that the vertical displacement increases rapidly with the vibration time increases at the beginning, and then it increases slowly. If the vibration time is over 5 hours, the vertical displacement at the top is 3 times as much as that at the bottom. From Fig. 10(b) we can see that the horizontal displacement becomes stable after some time. In the zone *x>2.0h*, the horizontal displacement is so small that it can be neglected. For an example, it is only 1/30 of that at *x=0* when loading lasts for over *5* hours. The development of both vertical and horizontal displacements is stable when loading lasts for some time.

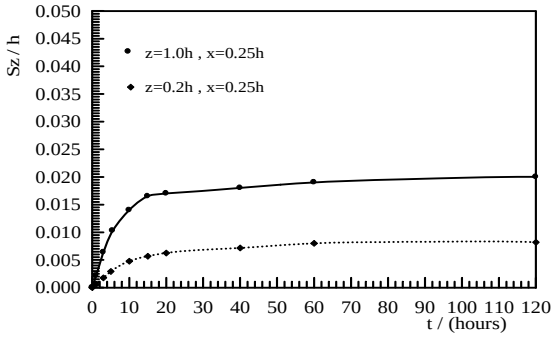

(a) *Sz/h~t*

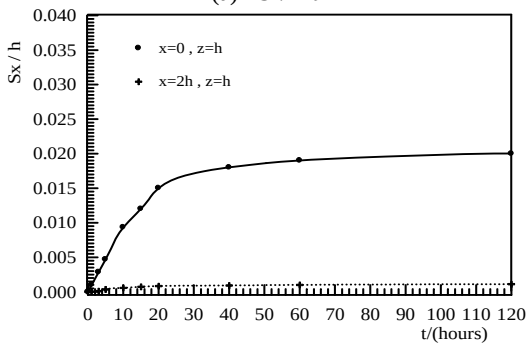

(b) *Sx/h~t*

Fig. 10 Development of displacement with vibration time

Effects of Factors on Deformation

Fig.11 shows that when the vibration time is 5 hours, effects of frequency and amplitude on the maximum vertical displacement at $x=0.25h$ and $z=h$. It is shown that the maximum vertical displacement at the surface of sediment decreases which may be caused by the low drainage under high frequency. The vertical displacement with the amplitude of 0.5*m* is 1.5 times that with the amplitude of 0.005*m*. Fig.12 shows that the effects of frequency and amplitude on the maximum horizontal displacement at $x=0$ and $z=h$ when the dynamic loading lasts for 5 hours. It can be seen that the maximum horizontal displacement increases with the decrease of frequency and the increase of amplitude. Fig.13 shows that the relationship between vertical or horizontal displacements and the elastic modulus of skeleton. It is shown that the vertical displacement and horizontal displacement reduce obviously with the increase of elastic modulus. When the modulus increases 10 times, the vertical and horizontal displacement both decrease about 2 times.

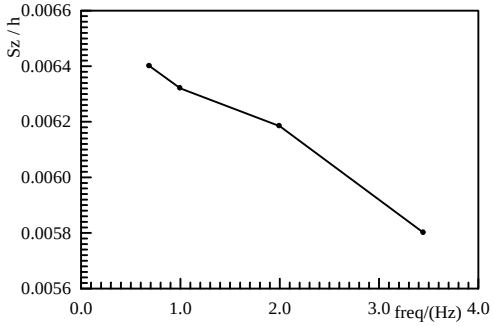

(a) *freq* ~s (*Sz*/*h*)

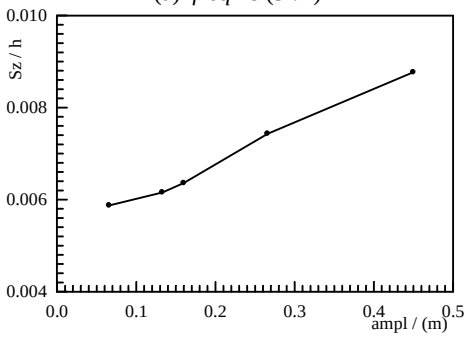

(b) *ampl* ~ (*Sz*/*h*)

Fig. 11 Effects of frequency and amplitude on the maximum vertical displacement

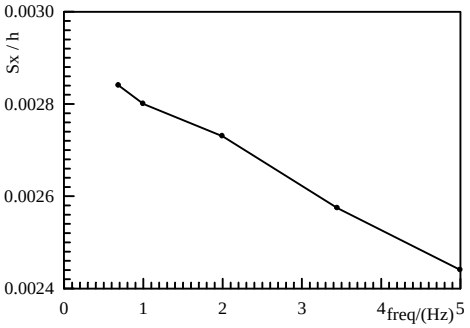

(a) *freq* ~ (*Sx*/*h*)

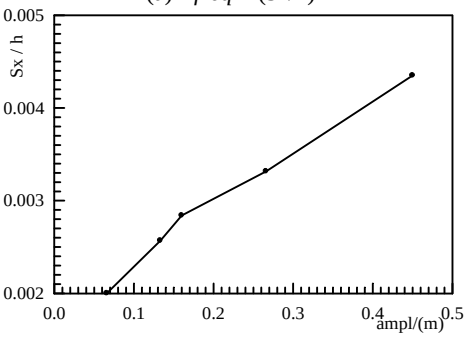

(b) *ampl* ~ (*Sx*/*h*)

Fig. 12 Effects of frequency and amplitude on the maximum horizontal displacement

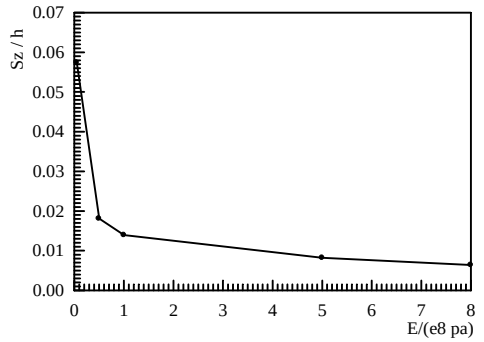

(a) $E \sim (Sz/h)$

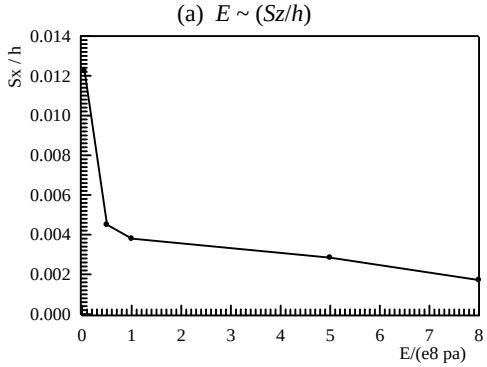

(b) $E \sim (Sx/h)$

Fig. 13 Effects of elastic modulus on the maximum displacement

CAPACITY DEGRADATION OF BUCKET FOUNDATION

Calculation Model

According to the centrifugal experiments and numerical results, a theoretical model is presented. The resistance of sediment is modeled by a series of nonlinear springs with different stiffness along the right side of bucket foundation. Furthermore, the horizontal damage and the bearing capacity of bucket foundation are described by *p-y* curves. The simplified calculation model is shown in Fig. 14.

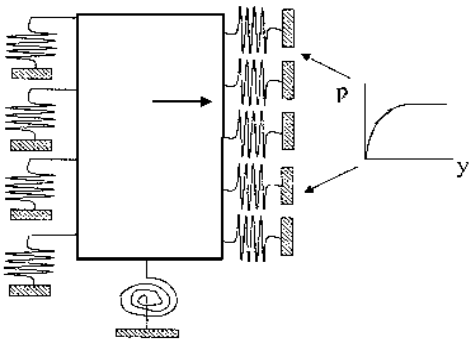

Fig.14 The spring model of bucket foundation

The stiffness coefficient is adopted as the sand sediment's elastic modulus E_0. The resistance at different depths on the right side of bucket is modeled by different spring stiffness coefficient which is taken as (1-*FL*) E_0 (*FL* is the liquefaction degree). The degradation degree is defined as the ratio of the capacity of bucket foundation in the sediment with some liquefaction degree to the initial bearing capacity.

Simulation Results

According to the centrifugal experiments, the bucket diameter is 0.5*m*; height 0.5*m*, wall thickness is $2\times10^{-3}m$ in simulating. The bucket material is steel whose elastic modulus is $2.1\times10^{11}pa$ and the Poisson's ratio is 0.25. The sand sediment's elastic modulus E_0 is $2.6\times10^{7}pa$. When the maximal horizontal displacement reaches 0.05*D* (*D* is the bucket diameter), the horizontal bearing capacity of bucket foundation is 4.4*kN* (Li and Wang, 2005).

According to the spring model, five horizontal springs are placed at the right side of bucket to simulate the horizontal resistance at different depths on bucket. The stiffness coefficient at different depth along the bucket side is (1-*FL*) E_0, the liquefaction degree from top to bottom of sand are 0.9，0.46，0.3，0.17，0.06 respectively. The horizontal bearing capacity of bucket foundation is 3.8*kN* according to the spring model. The degradation degree of bearing capacity of bucket foundation is 12% computed by spring model while it is 17% in centrifuge experiments (Lu et al., 2007). It indicates that the spring model can be used in the estimation of the bearing capacity of bucket foundations.

CONCLUSIONS

Based on centrifugal experimental results, numerical analysis using the software FLAC3D was carried out in this paper. The development of liquefaction in saturated sand around a bucket foundation is studied.

The expansion of liquefied zone and liquefaction degree and deformation under horizontal dynamic loading are studied. The effects of main factors are investigated. The development of liquefaction increases with the decrease of loading frequency and elastic modulus of skeleton and with the increase of amplitude. When the modulus increases 10 times, the vertical and horizontal displacement both decrease about 2 times.

A spring model for bucket foundation is adopted to investigate the capacity degradation of bucket foundation. The results obtained by the spring model are agreement well with the centrifugal experimental results.

ACKNOWLEDGEMENTS

This program is supported by the fund of Chinese Ocean Oil Co. and Chinese Academy of Sciences: KJCX2-SW-L03-01.

REFERENCES

Aas, PM and Andersen, KH (1992). "Skirted foundation for offshore structure," *Ninth Offshore South East Asia Conference*, Singapore, pp 1-7.

Andersen, KH (1988). "Bearing capacity for foundations with cyclic loads," *Journal of Geotechnical Engineering*, Vol 114, No 5, pp 540-555.

Andersen, KH and Dyvik, R (1993). "Field experiment of anchors in clay II: Predictions and interpretation," *Journal of Geotechnical Engineering*, Vol 119, No 10, pp 1514-1549.

Chi, LI, Jianhua, WANG, Zhenwen, LIU (2005). "Cyclic bearing capacity of single bucket foundation on soft clay sediment," *Journal of Geotechnical Engineering*, Vol 27, No 9, pp 1040-1044(in Chinese).

Chi, LI, Jianhua, WANG (2006). "Experimental Studies of Cyclic Bearing Capacity Character on Saturated Soft Clay Sediment," *Transactions of Tianjin University*, Vol 12, No 2, pp 137-141.

Chi, LI, Jianhua, WANG (2008). "Cyclic torsional slaear experimental studies on dynamic characters for saturated soft clay," *Rock and Soil Mechanics*, Vol 29, No 2, pp 460-464. (in Chinese).

David, NC (1982). "A sand model for the evaluation of displacement and

pore pressures in foundation of offshore gravity structures subjected to cyclic loading," *International Symposium on Numberical Models in Geomechanics*, pp 368-376.

Fast Lagrangian Analysis of Continua in 3 Dimensions (2005). Minnesota: Inc., *Itasca Consulting Group*.

Jianhong, ZHANG, Lanmin, ZHANG, Xiaobin, LU (2007). "Centrifuge modeling of suction bucket foundation for platforms under ice-sheet-induced cyclic lateral loadings," *Ocean Engineering* , Vol 34, pp 1069-1079.

Xiaobin, LU, Yingxiang, WU, Bingtian, JIAO. et al.(2007). "Centrifugal experimental study of suction bucket foundations under dynamic loading," *ACTA Mech*. Sinica., 23, pp.689-698.

Marr, WA (1981). "Permanent Displacements due to Cyclic Wave Loading," *J. of Geotechnical Engineering*, Vol 107, No GT8, pp 1129-1149.

Martin, GR, Finn, WDL and Seed, HB (1975). "Fundamentals of Liquefaction Under Cyclic Loading," *J. Geotech*., Div. ASCE, Vol 101, No GT5, pp 423-438.

Prevost, JH (1981). "Offshore gravity structures: Analysis," *Journal of Geotechnical Engineering*, Vol 107, No 2, pp 143-165.

Randolph, MF, House, AR (2002). "Analysis of Suction Cassion Capacity in Clay," *Proc Offshore Technology Conference*, OTC, Houston, Paper OTC 14236.

Sherif, L and Gharbawy EI (1999). "Suction Cassion in Soft Clay," *Proc. of the 18th International Conference on Offshore Mechanics and Arctic Engineering*, Newfoundland, Paper OFT 4063.

Tjelta, TL, Hermstad, J, Andenaes, E (1990). "The skirt piled gullfaks c platform installtion," *Proc Offshore Tech Conf*, OTC6473, pp. 453-462.

Xiaobing, LU, Peng, CUI (2004). "The liquefaction and displacement of highly saturated sand under water pressure oscillation," *Ocean Engineering*, Vol 31, No 7, pp 795-811.

Yihua, WANG, Xiaobing, LU, Shuyun WANG (2006). "The response of bucket foundation under horizontal dynamic loading," *Ocean Engineering* , Vol 33, pp 964-973.